Neuron, Vol. 25, 549–561, March, 2000, Copyright ©2000 by Cell Press

atonal Regulates Neurite Arborization but Does Not Act as a Proneural Gene in the *Drosophila* Brain

Bassem A. Hassan,*†# Nessan A. Bermingham,*†§ Yuchun He,*† Yan Sun,*‖ Yuh-Nung Jan,*‖ Huda Y. Zoghbi,*†‡§ and Hugo J. Bellen*†‡#
*Howard Hughes Medical Institute
†Department of Human and Molecular Genetics
‡Program in Developmental Biology
§Department of Pediatrics
Baylor College of Medicine
Houston, Texas 77030
‖Department of Physiology and Biochemistry
University of California, San Francisco
San Francisco, California 94143

Summary

***Drosophila atonal* (*ato*) is the proneural gene of the chordotonal organs (CHOs) in the peripheral nervous system (PNS) and the larval and adult photoreceptor organs. Here, we show that *ato* is expressed at multiple stages during the development of a lineage of central brain neurons that innervate the optic lobes and are required for eclosion. A novel fate mapping approach shows that *ato* is expressed in the embryonic precursors of these neurons and that its expression is reactivated in third instar larvae (L3). In contrast to its function in the PNS, *ato* does not act as a proneural gene in the embryonic brain. Instead, *ato* performs a novel function, regulating arborization during larval and pupal development by interacting with *Notch*.**

Introduction

The *Drosophila* gene *atonal* (*ato*) defines a family of genes involved in nervous system development from *Caenorhabditis elegans* to man (Jarman et al., 1993; Akazawa et al., 1995; Zhao and Emmons, 1995; Ben-Arie et al., 1996). *ato* was initially described as a proneural gene that is necessary and sufficient for the development of the *Drosophila* chordotonal organs (CHOs) (Jarman et al., 1993), a group of internal mechanoreceptors in the peripheral nervous system (PNS) thought to be involved in proprioception (Moulins, 1976; McIver, 1985). CHOs are found beneath the cuticle in thorax and abdomen, in joints of legs and wings, and in a pocket of the second antennal segment. In the antenna, CHOs are required for near hearing (Dreller and Kirschner, 1993; Eberl, 1999) and geotaxis (B. A. H. and H. J. B., unpublished data). In addition to its requirement to specify CHO, *ato* was also shown to be required for the development of the founder photoreceptor cells of the *Drosophila* retina (Jarman et al., 1994, 1995). Mutations in *ato* result in flies that lack CHOs and eyes and that have severely reduced optic lobes (Jarman et al., 1993, 1995). More recently, *ato* was also shown to be essential for the development of the Bolwig organ, the *Drosophila* larval photoreceptor organ (Daniel et al., 1999). Thus, *ato* has been shown to be a proneural gene in both the PNS and the visual system. In its function as a proneural gene in the PNS, *ato* interacts with genes in two pathways: the *Notch* pathway and the epidermal growth factor receptor (EGFR) pathway. The EGFR pathway is used by *ato* to recruit additional precursor cells from surrounding epidermal cells (Okabe and Okano, 1997; zur Lage et al., 1997; zur Lage and Jarman, 1999). In contrast, *Notch* appears to antagonize *ato* function by limiting the number of epidermal cells permitted to adopt the CHO precursor fate (zur Lage and Jarman, 1999).

Although at least five mouse *ato* homologs (MATHs) have been identified (Takebayashi et al., 1997; Ben-Arie et al., 2000), *Math1* and *Math5* are arguably the only true mouse homologs of *ato*. They share 67% and 74% amino acid sequence identity in their basic helix–loop–helix (bHLH) domain with ATO, respectively, and 100% identity in the basic DNA binding domain (Akazawa et al., 1995; Ben-Arie et al., 1996). *Math5* is expressed in photoreceptor cells in the mouse retina, but little is known about its requirement in eye development (Brown et al., 1998). *Math1* is expressed in mechanoreceptor cells in the skin, the hair cells of the inner ear, and the articular cartilage of the joints, a pattern remarkably similar to that of *ato* (Bermingham et al., 1999; Ben-Arie et al., 2000). In addition, *Math1* is expressed in the spinal cord, the brain stem, and the cerebellum (Akazawa et al., 1995; Ben-Arie et al., 1996, 2000). Loss of *Math1* function results in the loss of the cerebellar external granular layer and of the inner ear mechanosensory hair cells (Ben-Arie et al., 1997; Bermingham et al., 1999).

ato expression in the *Drosophila* brain has been reported previously (Jarman et al., 1993; Sun et al., 1998; Ben-Arie et al., 2000), but neither the identity of the cells expressing *ato* nor their function has been determined. In contrast to the relatively detailed anatomical studies available for the *Drosophila* adult brain and optic lobes (Strausfeld, 1976; Bausenwein et al., 1992; Yang et al., 1995), the molecular and cellular mechanisms underlying their development remain poorly understood. In addition, very few genes have been assigned precise functions during brain development. Finally, while the loss of central brain regions has been shown to underlie various behavioral defects in specific mutants (Strauss and Heisenberg, 1993), these lesions are often too extensive to uncover the requirements of specific groups of cells. Hence, the functions of many central brain structures or groups of neurons of the adult fly are unknown.

The functional properties of neurons derive from their interactions with their targets. The proper arborization pattern of axons is key not only in establishing the appropriate synaptic contacts among neurons and between neurons and effector cells but also in mediating neuronal plasticity, which underlies important aspects of behavior (reviewed by Kolb and Whishaw, 1998). While significant advances have been made in understanding the molecules that control axon guidance (reviewed by Tessier-Lavigne and Goodman, 1996; Nieto, 1996), very little

To whom correspondence should be addressed (e-mail: bhassan@bcm.tmc.edu [B. A. H.], hbellen@bcm.tmc.edu [H. J. B.]).

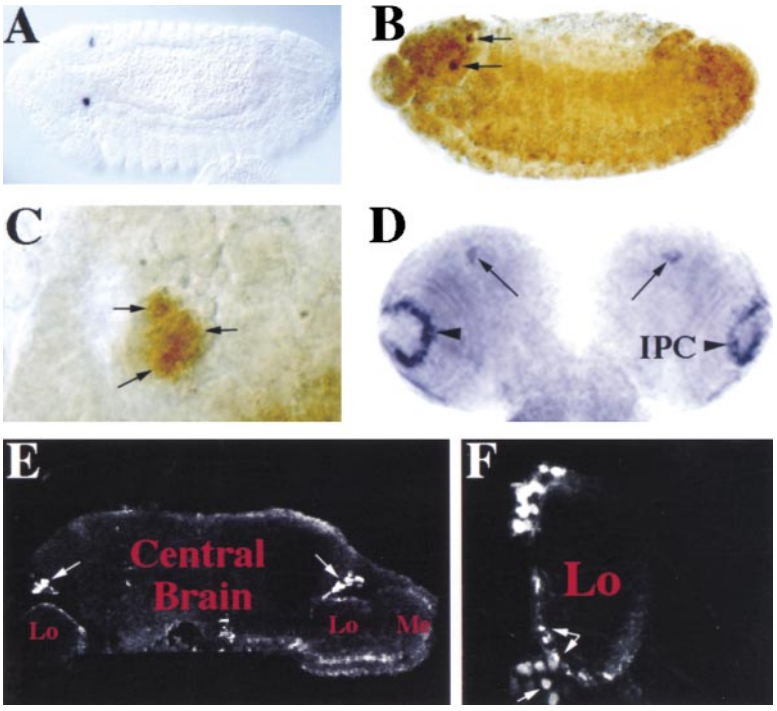

Figure 1. *ato* Is Expressed in the Central Brain at Multiple Developmental Stages

(A) Dorsal view of a stage 13 *Drosophila* embryo hybridized with a riboprobe for the *ATO* RNA. *ATO* expression is detected in two small (3–5 cells) clusters in the dorsal central brain (one in each hemisphere).

(B) A lateral view of a similar stage embryo showing the expression of the ATO protein in the same clusters, detected with a new guinea pig polyclonal antibody (GP50).

(C) A high-magnification view of a stage 13 embryonic brain showing ATO expression in 3 cells (arrows), which, from their size, appear to be ganglion mother cells rather than neuroblasts. One or two more cells within the cluster are visible in a different focal plane.

(D) An L3 brain hybridized with the *ATO* riboprobe. Expression is detected in the inner proliferation center (IPC) of the optic lobes (horseshoe-like expression) and in two clusters of 20–30 cells in each of the two central brain hemispheres (arrows).

(E) A cryosection of an adult *Drosophila* brain stained with GP50. ATO expression is detected in two clusters of about 30 cells in the dorso–lateral region of the central brain (arrows) immediately adjacent to the lobula.

(F) A high-magnification view of another section stained with the same antibody shows that ATO is also expressed in a group of cells in the ventro–lateral brain (arrows). Abbreviations: Lo, lobula complex, and Me, medulla.

is known about the genes and pathways that regulate branching and arborization. Here, we report that *ato* marks a set of three neuronal clusters that project bilaterally onto the optic lobes in the adult brain. To our knowledge, these clusters and their projections have not been described previously. Using a novel fate mapping strategy based on the *UAS-Gal4* system, we show that *ato* is expressed in the embryonic precursors of one of the clusters. Unlike in the PNS and the retina, *ato* is not acting as a proneural gene in the central brain. We show that *ato* is required for proper axon branching and arborization and is antagonized by *Notch*. We find that loss of these neurons or their failure to innervate their targets results in failure to eclose from the pupal case. In summary, we have uncovered a group of *Drosophila* brain neurons and described novel functions for *ato* in neuronal development and neurite arborization.

Results

ato Is Expressed in the Embryonic, Larval, and Adult Brain

To examine the profile of *ato* expression in the *Drosophila* central brain, we performed in situ hybridization and immunohistochemistry experiments on embryos, third instar larval (L3), and adult brains (Figure 1). In stage 13 embryos, two small clusters of cells express the *ATO* RNA (Figure 1A). These cells are located in the dorso–lateral region of the central brain, proximal to the developing optic lobes. This expression is very transient, and no *ATO* RNA is detectable in these cells after stage 13 or in similar positions in first (L1) or second (L2) instar larvae. Using a new antibody against the ATO protein (Experimental Procedures) we find that ATO has an expression pattern identical to that of *ATO* RNA (Figure 1B). The *ATO*-expressing clusters are composed of 3–5 cells in each brain hemisphere (Figure 1C). The sizes of the cells suggests that at least one is a neuroblast, whereas the others are likely to be ganglion mother cells. During early larval development, the *ATO* RNA is detectable in the inner proliferation zone of the optic lobes, but no expression is detected in the central brain in L1 and L2 (data not shown). In L3 *ATO*, RNA is once again detectable in the central brain in two clusters comprised of 20–30 cells in the dorso–lateral region (Figure 1D, arrows) proximal to the optic lobe. In addition, the inner proliferation zone of the optic lobe continues to express *ATO* RNA (Figure 1D, arrowheads). Immunohistochemistry on frozen adult head sections showed that ATO is expressed symmetrically in one dorsal cluster (DC) of cells adjacent to the lobula in each brain hemisphere (Figure 1E, arrows), as well as in two small groups of ventral cells (Figure 1F, arrows). In summary, ATO is transiently expressed in stage 13 embryos in the brain. Expression is reinitiated in a cluster of neurons in the L3 brain and observed in three clusters of neurons of the adult brain.

The *ato* Brain Enhancer Recapitulates *ato* Expression

To gain a better understanding of the origin of the ATO-expressing neurons, and of the function of *ato* in the brain, we identified an enhancer fragment that recapitulates *ato* expression (Figures 2A and 2B). Sun et al. (1998) identified a 5.6 kb regulatory fragment directly

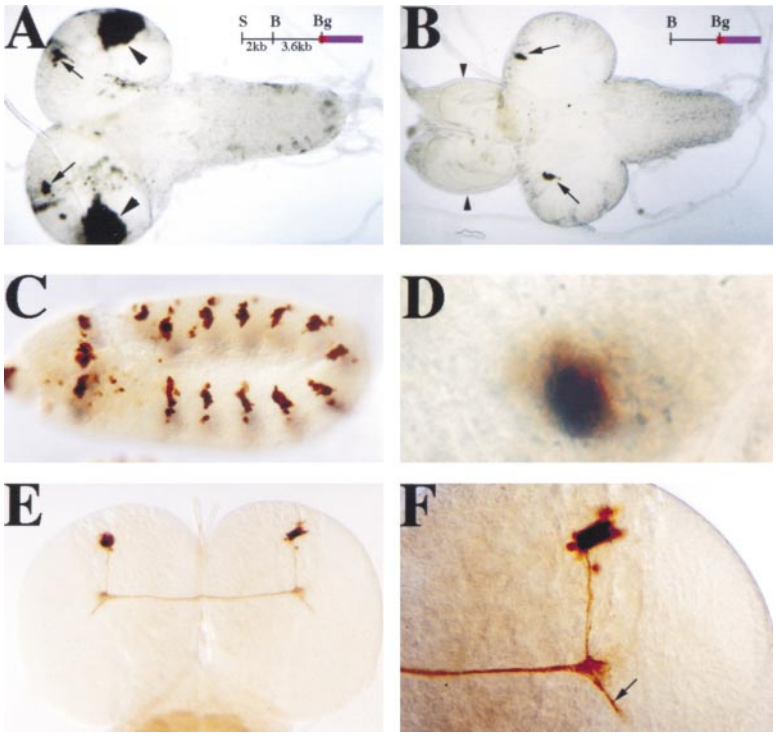

Figure 2. The *ato* Brain Enhancer Mimics *ato* Expression in Embryos and Larvae

(A) A dorsal view of an L3 brain from a transgenic animal carrying a construct in which 5.6 kb of genomic DNA directly upstream of the *ato* ORF drives an *ato-lacZ* (nuclear form) fusion reporter. The red color indicates *ato* sequences, and the blue indicates *lacZ* sequences. Abbreviations: S, SmaI; B, BamHI; and Bg, BglII. The brain was stained with a monoclonal antibody (Promega) for β-gal. Expression is detected in the inner proliferation center (strong staining on either side), as well as in the central brain clusters (arrows).

(B) An L3 brain and a pair of leg discs (arrowheads) from a transgenic animal carrying a construct in which 3.6 kb of genomic DNA directly upstream of the *ato* ORF drives an *ato-lacZ* fusion reporter. β-gal expression is detected only in the central brain clusters (arrows).

(C) A lateral view of a stage 11 transgenic embryo carrying a construct in which the 3.6 kb BamHI-BglII fragment drives a *Gal4* protein (*ato-Gal4*) and a *UAS-lacZ* (cytoplasmic form) construct. The embryo was stained for β-gal expression, which is detected in the PNS CHO precursors.

(D) A high-magnification view of the brain of a stage 13 *ato-Gal4/UAS-lacZ* embryo showing β-gal expression in a central brain cluster.

(E) A dorsal view of an L3 brain from an *ato-Gal4/UAS-lacZ* animal. β-gal expression is detected in two clusters of 20–30 neurons with a commissure bridging the two brain hemispheres. A bundle of fibers extends out of each commissure into the developing optic lobes.

(F) A high-magnification view of the right hemisphere of the same brain, showing that the neurons extend a bundle of axons ventrally through the brain. These axons make a 90°C turn toward the left hemisphere, thus forming the commissure. Axons arriving from the left hemisphere exit the commissure at a 45°C angle to enter the developing optic lobes.

upstream of the *ato* open reading frame (ORF) as sufficient for *ato* expression in the embryonic PNS as well as in the L3 leg, antennal, and wing discs. We find that this fragment also directs *lacZ* expression to the larval optic lobes and central brain (Figure 2A). However, a 3.6 kb fragment directly upstream of the *ato* ORF directs expression exclusively to the central brain clusters in L3 (Figure 2B, arrows). No expression was observed with the 3.6 kb enhancer in imaginal discs or other areas of the CNS, but it directs *lacZ* expression in the embryonic CHO precursors (Sun et al., 1998).

To further characterize the cells that express *ato*, the 3.6 kb enhancer was cloned upstream of *Gal4*, and two independent transgenic lines were generated (*ato-Gal4* 14a and *ato-Gal4* 10). We analyzed the expression of both lines throughout fly development to determine whether they mimic *ato* expression. *ato-Gal4* is initially expressed in the sensory organ precursors of the embryonic CHOs (Figure 2C). At stage 13, 3–5 cells in each brain hemisphere initiate *ato-Gal4* expression (Figure 2D). While *lacZ* expression lasts longer than does *ATO* RNA, it is nonetheless transient and is no longer detectable in stage 15 embryos (see below). However, *lacZ* expression is reinitiated at L3 in a cluster of 25–30 neurons in each brain lobe (Figures 2E and 2F). Each cluster of neurons sends a bundle of axons ventrally and then contralaterally toward the opposite optic lobes. At the junction between the central brain and the developing lobula, the axons derived from the contralateral cluster branch out of the commissure, into the developing optic lobes (Figure 2F, arrow). These data indicate the 3.6 kb fragment recapitulates the expression of *ato* in embryos and larvae.

As ATO is expressed in adult brains (Figures 1E and 1F), we stained *ato-Gal4/UAS-lacZ* adult brains with anti-β-galactosidase (anti-β-gal) and analyzed the data with confocal microscopy. In adult flies, *ato-Gal4* is expressed in a DC and in two ventral clusters (VCs: VLC and VBC) of neurons (Figures 3A and 3D). As shown in Figure 3B, some axons of the DC project ipsilaterally over the lobula. However, most axons of the DC form a bundle that is a component of the dorsal commissure (Strausfeld, 1976) and project contralaterally toward the lobula complex and the medulla (Figures 3A–3D). These neurites fan out over the lobula complex and the inner chiasm. Ten to twelve tracts cross the outer chiasm, toward the medulla, in a ladder-like pattern (Figure 3C). Over the medulla, the fibers branch and appear to contact one another to form a "grid-like" lattice (Figure 3D). No fibers cross the lamina.

The ventral brain cluster (VBC) appears to be located in the central brain, while the ventral lobular cluster (VLC) is located in the lobula. The axons of the VBC project along the brain–lobula border toward the DC, while the VLC forms an extensive network of fibers in the ventral lobula (Figure 3D). To determine when the expression of *ato* is initiated in the VCs, we examined pupal brains at 50% and 75% pupal development (data not shown). All clusters express *ato-Gal4* at both stages, suggesting that *ato* expression in the DC never ceases after L3 and

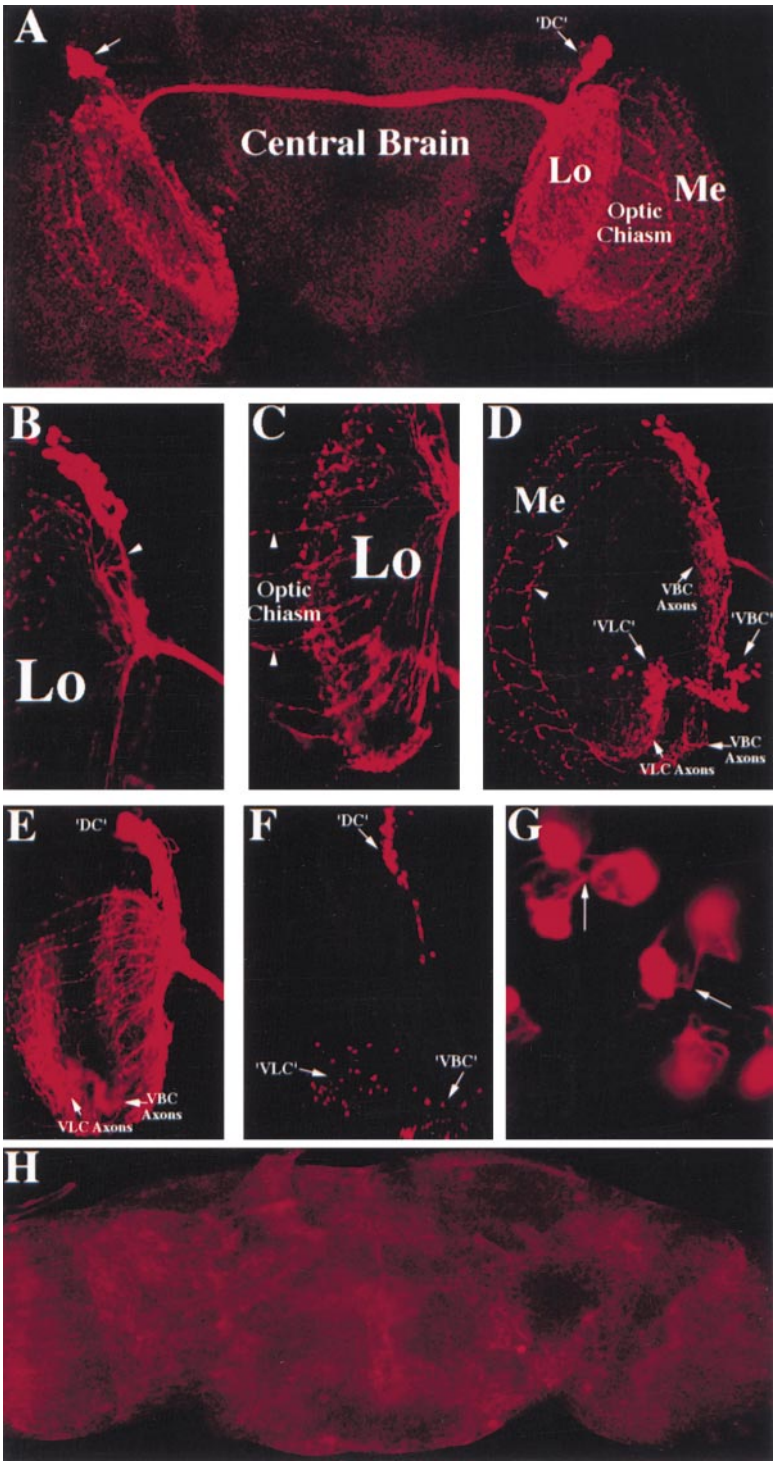

Figure 3. The *ato* Brain Enhancer Mimics *ato* Expression in Adults

(A) A confocal section of a whole-mount adult brain from an *ato-Gal4/UAS-lacZ* transgenic animal stained for β-gal expression. Expression is detected in the two DCs (arrows), as well as in groups of ventral cells. The commissure is also visible, as is the elaborate innervation pattern of the optic lobes by the *ato* neurons.

(B) A high-magnification confocal section through a DC, showing the descending bundle of axons, as well as fibers running between the cluster and the dorsal lobula (arrowhead).

(C) A high-magnification confocal section through the lobula, revealing the innervation pattern formed by the axons exiting the commissure. Note the regular spacing between the major fibers, forming a fan-shaped pattern. Major fibers (10–12) exit the lobula and cross the optic chiasma toward the medulla (arrowheads), forming a regular array in a ladder-like pattern.

(D) A high-magnification confocal section through the ventral cells and the medulla. The ventral cells are divided into two clusters (arrows). One cluster is in the brain (VBC), while the other is in the lobula (VLC). VBC axons innervate the brain lobula border, whereas VLC axons form a dense network of fibers in the ventral lobula that also appears to extend toward the medulla. The medulla is also innervated by the a grid-like pattern of fibers generated by the branching (arrowheads) of the axons that cross the optic chiasma.

(E) A confocal section of a whole-mount adult brain from an *ato-Gal4/UAS-tau.lacZ* transgenic animal stained for β-gal expression to reveal the axonal pattern. The staining labels the fibers over the optic lobes, showing that the innervation patterns seen in (A) through (D) are due to axons.

(F) A confocal section of a whole-mount adult brain from an *ato-Gal4/UAS-Nod.lacZ* transgenic animal stained for β-gal expression to reveal the dendritic pattern. Note that no arborization is visible over the optic lobes, confirming that the optic lobe innervation by the *ato*-expressing neurons is axonal and not dendritic.

(G) A high-magnification view of a confocal section through the DC of the same brain, showing that DC neurons have multiple dendritic projections that appear to contact each other (arrows).

(H) A confocal section of a whole-mount adult brain from a *UAS-reaper/+;ato-Gal4,UAS-lacZ/+* transgenic animal stained for β-gal expression. No β-gal expression is detected, indicating that *reaper* expression completely eliminated the *ato*-expressing neurons.

that VLC and VBC initiate *ato* expression de novo during pupal development.

To confirm that the arborization patterns observed with cytoplasmic *lacZ* reflect axonal projections, we used the axonal marker *UAS-tau.lacZ*, which is driven by *ato-Gal4*. We find that *tau.lacZ* expression mimics that of cytoplasmic *lacZ*, revealing the arborizations in the lobula and medulla (Figure 3E). Thus, it appears that the arborizations of the DC and VC neurons in the optic lobes are composed of axons, implying that the *ato*-expressing neurons output onto the optic lobes rather than receive input from them. The dendritic projections of these clusters were examined using *UAS-Nod.lacZ*, which has been shown to be localized to dendrites (Clark

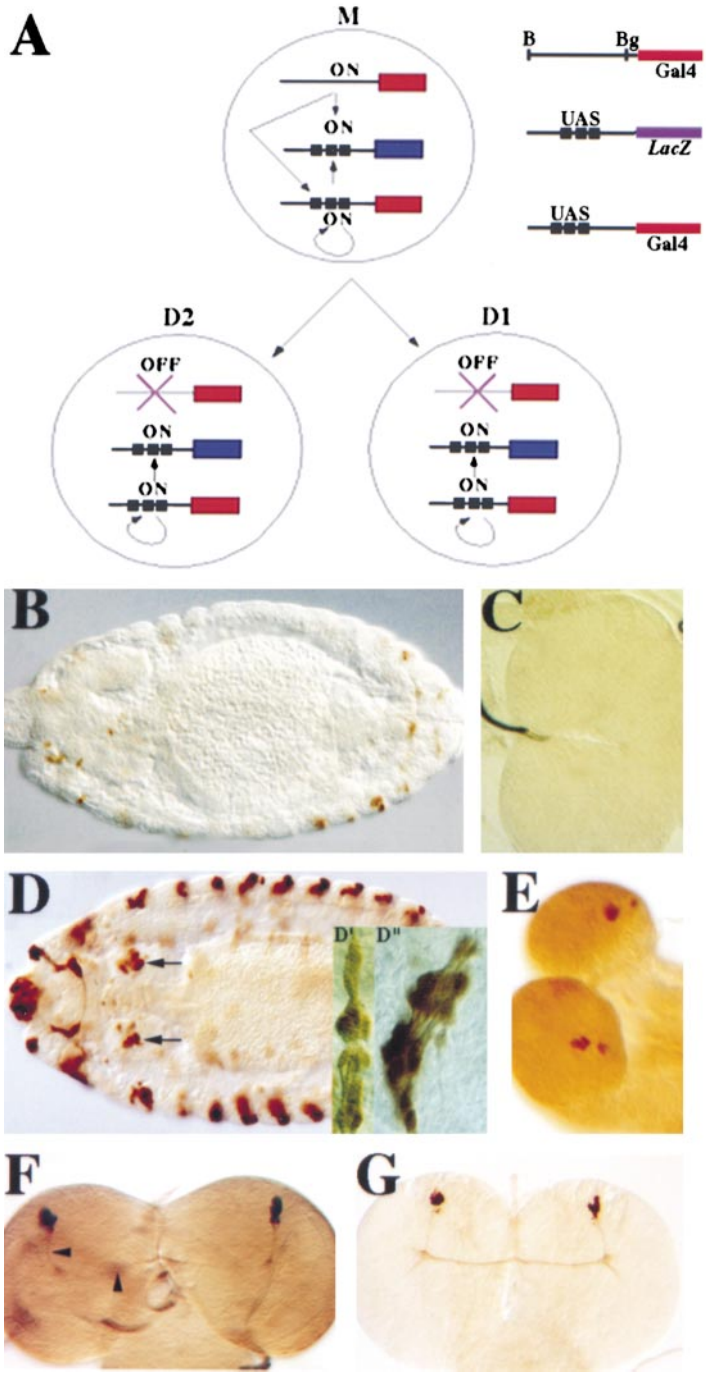

Figure 4. A Novel Method for Fate Mapping Applied to the *ato*-Expressing Cells

(A) A schematic of a novel method for fate mapping and signal amplification. A combination of an *enhancer-Gal4* construct with a *UAS-Gal4* construct and a UAS-Reporter construct can result in lineage tracing. In the mother cell (M), the precursor-specific enhancer activates *Gal4* expression. This results in the synthesis of *Gal4* protein, which will bind to its activation sites (closed squares) upstream of the *UAS-Gal4* and *UAS-lacZ* constructs. This, in turn, results in the synthesis of large amounts of *Gal4* and reporter proteins. In the daughter cells (D1, D2), the precursor-specific enhancer is off. However, *Gal4* protein inherited from the mother cell activates the *UAS-Gal4* and *UAS-lacZ* constructs to reinitiate the cycle.

(B and C) Dorsal views of *ato-Gal4/UAS-lacZ* transgenic stage 15 embryo (B) and late L1 brain (C) stained for β-gal expression. No expression is detected in the brain.

(D–G) Dorsal views of *UAS-Gal4;ato-Gal4/UAS-lacZ* transgenic stage 15 embryo (D), L1 (E), late L2 (F), and L3 (G) brains stained for β-gal expression. The DC (arrows, [D]) can be followed from embryos to L3. In addition, the expression of *ato-Gal4* in the PNS CHO precursors results in the labeling of the thoracic (D′) and abdominal (D") CHOs in stage 15 embryos. At L2, a faint commissure is already visible (arrowheads, [F]).

et al., 1997). As shown in Figures 3F and 3G, the dendrites of the clusters are very short and connect to each other, forming dendrodendritic connections. These data indicate that the *ato*-expressing neurons are multipolar, unlike most neurons of the insect brain.

The above data raise several questions. First, are the clusters of the adult brain derived from *ato*-expressing embryonic precursors? Second, what is the role of *ato* in embryonic precursors? Third, is the expression of *ato* required in L3 and adults? And fourth, what is the function of the *ato*-expressing clusters of neurons? To answer these questions, we took advantage of the viability of *ato* mutants (Jarman et al., 1995), allowing us to examine the presence and morphology of these neurons at various stages. We also employed the *ato* brain enhancer to (1) mark these neurons and (2) express a variety of gene products.

ato Is Reactivated within the Same Lineage in the Dorsal Brain

To address the relationship between the *ato*-expressing precursor cells in the embryonic brain and the *ato*-

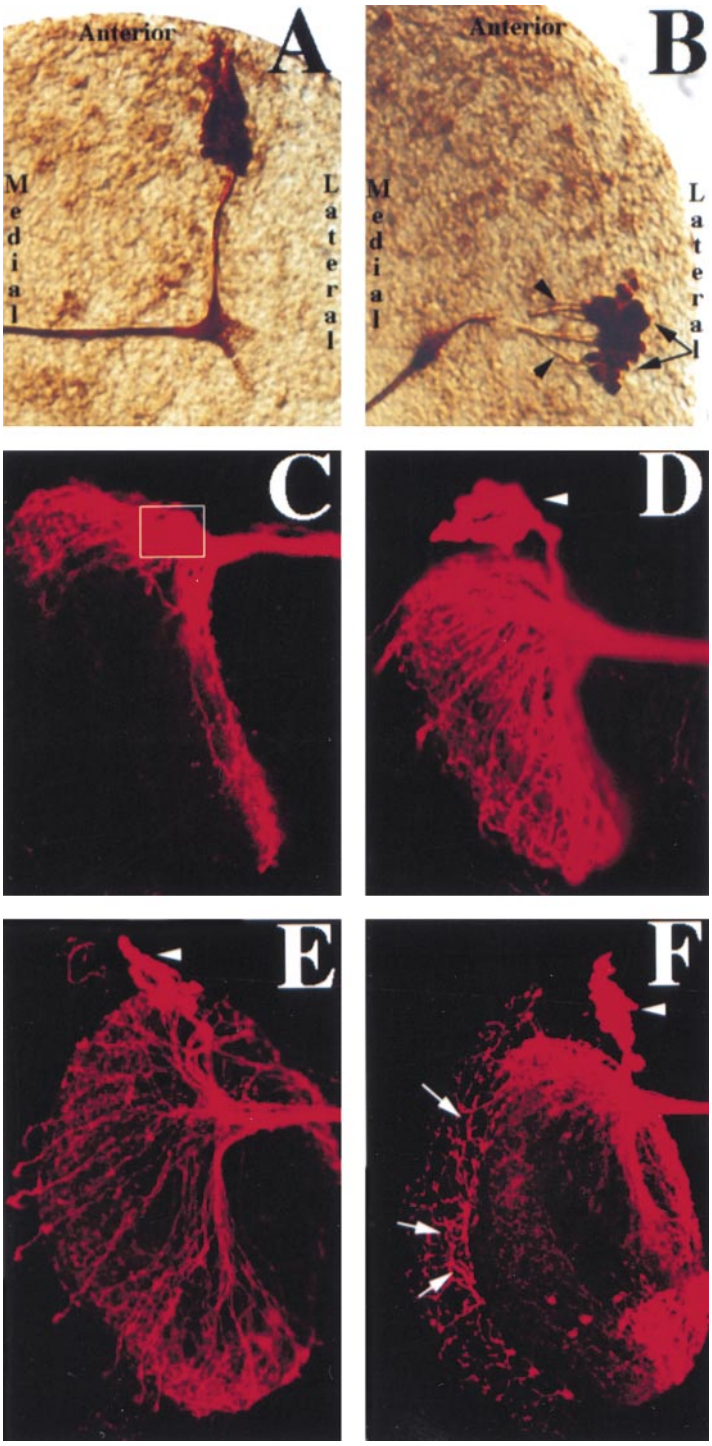

Figure 5. *ato* Is Required for Differentiation and Axon Branching

(A) A *UAS-lacZ;ato-Gal4,ato^{1}/TM6* L3 brain stained for β-gal expression. Note the normal positioning and clustering of the DC neurons, as well as the fasiculated bundle of descending axons.

(B) A *UAS-lacZ;ato-Gal4,ato^{1}/Df(3R)p13* L3 brain stained for β-gal expression. The positioning of the DC is abnormal, and the cells appear to be less tightly clustered (arrows). In addition, the axons are clearly defasiculated (arrowheads).

(C) A confocal section through a *UAS-lacZ; ato-Gal4,ato^{1}/Df(3R)p13* adult brain stained for β-gal expression. The position of the DC is abnormal (box), and the innervation of the lobula is severely diminished.

(D) A confocal section through a *UAS-ato/ UAS-lacZ;ato^{1},ato-Gal4/Df(3R)p13* adult brain stained for β-gal expression, showing the rescue of the innervation of the lobula and the position of the cluster (arrowhead).

(E) A confocal section through a *UAS-ato/+; ato-Gal4,UAS-lacZ* adult brain stained for β-gal expression. The *UAS-ato* line expresses high levels of ATO (Jarman and Ahmed, 1998). The positioning of the DC is unaffected (arrowhead), but the innervation of the lobula is more extensive than wild-type due to excessive branching (compare with Figure 3C).

(F) A different confocal section through the same brain as in (E), showing the excessive branching (arrows) over the medulla resulting in the disruption of the regular grid-like pattern (compare with Figure 3D).

expressing neurons in the L3 and adult brain, we fate mapped the progeny of the embryonic precursors expressing *ato* using a novel approach based on the *UAS-Gal4* system (Brand and Perrimon, 1993), which introduces an amplification step between the *ato-Gal4* and the *UAS-lacZ* steps via a *UAS-Gal4* construct (Figure 4A). The rationale of the methodology is as follows: the *ato-Gal4* construct is used to activate the expression of the *Gal4* protein in a precursor-specific manner. *Gal4* binds to the *UAS* sites of the *UAS-lacZ* and *UAS-Gal4* constructs. Extra *Gal4* protein from the *UAS-Gal4* construct binds to the *UAS* sites upstream of *lacZ* and autoactivates *Gal4* production. Hence, the signal becomes self-propagating and is substantially amplified. Upon cell division, daughter cells inherit sufficient *Gal4* protein to reactivate the cascade.

We applied this strategy to the *ato* brain enhancer. Normally, expression of *ato-Gal4* is no longer detectable by stage 15 (Figure 4B) and is absent throughout early larval development (L1 and L2) (Figure 4C). In contrast,

when the *UAS-Gal4* construct is introduced, the lineage can be easily followed with anti-β-gal antibodies. At stage 15 (Figure 4D, arrow), the two brain clusters consist of about 8 cells each. In addition, specific PNS organs are strongly positive for β-gal. These organs all correspond to the embryonic CHOs (Figures 4D′ and D′′), in agreement with the expression of *ato-Gal4* in the CHO precursor cells. In L1 brains (Figure 4E), there are ~10 cells in each cluster that consist of two small subclusters. In late L2 (Figure 4F), each cluster comprises about 16 cells, and a thin commissure can already be seen (arrowheads). In L3, a single cluster of 25–30 cells can be observed in each brain lobe (Figure 4G), the same number observed without the *UAS-Gal4* construct (Figure 2E). Had the embryonic precursors given rise to a different set of neurons, two or more clusters of neurons would have been identified in L3. We did not observe any other clusters in L1–L3 brains. We therefore conclude that the DC is derived from the *ato*-expressing embryonic brain cells. Studies using other promoter/enhancer *Gal4* constructs indicate that this fate mapping method may be generally applicable (B. A. H. and H. J. B., unpublished data).

Precursor Differentiation and Axon Arborization: Two Distinct Roles for *ato* in Brain Development

What might the function(s) of *ato* be in the central brain? To address this question, we examined the consequences of the loss and gain of *ato* function in the DC in L3 and adult brains using the *ato-Gal4* line as a marker and a driver. Surprisingly, we find that all three clusters (DC, VBC, VLC) are present in brains homozygous for the ato^1 allele (Jarman et al., 1995; data not shown) as well as in brains transheterozygous for ato^1 and a deficiency that uncovers the *ato* region (*Df[3R]p13*) (Jarman et al., 1993) (Figure 5). However, several defects are obvious in *ato* mutant brains. While heterozygous control L3 brains show a normal DC (Figure 5A), mutant L3 brains show severe defects in DC position and organization (Figure 5B, arrows). In addition, probably as a result of the loose morphology of the cluster, the descending axon bundles are defasiculated (Figure 5B, arrowheads). These defects were observed with about 15% penetrance and suggest a weak or partially redundant differentiation requirement for *ato* in the precursors of the DC lineage. Note, however, that the DC axons form a commissural tract, strongly suggesting that their basic identity as commissural neurons is not affected by the *ato* mutation.

To investigate if *ato* is required in the postmitotic DC neurons, as the reinitiation of its expression suggests, we examined the morphology of the axonal projections of the DC neurons of adult *ato* mutant brains. The DC forms a stereotypical axonal pattern, making it simple to detect aberrations that may be caused by the *ato* mutation. In adult brains, we find that in addition to the aberrant positioning of the cluster seen in L3 (Figure 5C, box), the arborization pattern of the DC over the lobula is severely impaired in $ato^1/Df(3R)p13$ flies (Figure 5C). Most axons enter the lobula either ventrally or dorsally and show very limited branching, failing to form a proper "fan-shaped" pattern. Since *ato* mutant brains have a severely reduced medulla (Jarman et al., 1994), we were unable to examine the medullar part of the pattern. While these data suggest a role for *ato* in axon arborization, alternative interpretations are possible. First, the observed axonal defects may be caused by the significant loss of optic lobe structures associated with loss of *ato* function (no lamina or medulla, reduced lobula). Second, it is possible that the defects are a reflection of the improper differentiation of the DC cells rather than a reflection of a specific role for *ato* in arborization.

To rule out the first possibility, we examined the lobular innervation pattern of the DC in *sine oculis* (*so*) mutant brains. *so* mutants lack eyes and a lamina, and exhibit a severely reduced medulla and a reduced lobula (Fischbach, 1981). In gross morphology and size, *so* brains and *ato* brains are indistinguishable. As *so* mutants show variability in phenotypic penetrance, only flies that completely lack eyes were used. We find that the axonal projections of the DC lobular pattern appears essentially wild-type in *so* mutant brains (data not shown), indicating that the axonal defects in the *ato* mutant brains are due to the *ato* mutation. To demonstrate that this is indeed the case, we expressed *ato* using the *ato-Gal4* driver in $ato^1/Df(3R)p13$ flies. This resulted in a rescue of the lobular innervation pattern (Figure 5D). This indicates that the role of *ato* in DC axon arborization is specific and cell autonomous.

Finally, if *ato* does play a role in the development of the axonal pattern of the DC neurons, its overexpression in these neurons may result in an aberrant axonal pattern without affecting the number or position of the DC neurons. We used the *ato-Gal4* line to overexpress *ato* in the DC and marked the cells simultaneously using *UAS-ato* and *UAS-lacZ* constructs. Consistent with a role for *ato* in neurite arborization, we find excessive branching in the lobula (Figure 5E) and the medulla (Figure 5F) as compared with the wild-type patterns in Figures 3C and 3D, respectively. Importantly, the organization of the cluster, its size, and its position are unaffected in L3 brains (data not shown) and adult brains (Figures 5E and 5F, arrowheads). In addition, the number of axons crossing the optic chiasma, though not their morphology, is wild-type (data not shown). These data strongly suggest that the early differentiation of the cluster is unaffected when *ato* is overexpressed. We conclude that the axonal defects observed in *ato* loss- and gain-of-function experiments reflect a specific requirement for *ato* in the control of the arborization pattern of the DC neurons.

Notch Antagonizes the Arborization Function of *ato*

To understand the mechanism by which *ato* functions in axonal development, we examined the role of *Notch* in the development of the DC axonal pattern. Two observations make *Notch* a logical candidate. First, *ato* and *Notch* interact in an antagonistic fashion during CHO development. For example, in the leg femoral CHO, gain of *Notch* function reduces the number of precursors selected from the *ato*-expressing proneural cluster (zur Lage and Jarman, 1999). Second, *Notch* has been shown to be required for axon guidance, perhaps mediating axon–substrate interactions, in both the PNS and CNS (Giniger et al., 1993; Giniger, 1998). If *ato* and *Notch* act antagonistically in arborization, it is expected that

Notch activity levels would be relatively low within the DC, where its function is repressed by *ato*, and relatively high in the substrate cells, where *ato* does not antagonize it. Thus, after *ato* expression is reinitiated in the DC neurons, a differential in *Notch* activity levels may occur between the arborizing axon and the substrate cells. Perturbations of this imbalance, either by raising *Notch* activity levels in the DC or by reducing them in the surrounding cells, may result in defective arborization patterns. This model allows for three specific predictions. First, the generalized loss of *Notch* function may result in excessive arborization of the DC neurons, whereas the DC-specific loss of function would cause no significant defects. Second, the gain of *Notch* in the DC neurons is expected to inhibit arborization. Third, if the activation of *ato* in the DC neurons serves to antagonize *Notch* activity, then it is expected that the gain of *Notch* function will be epistatic to the gain of *ato* function.

To examine the requirements for *Notch* in DC axon development, we used two *Notch* alleles: a temperature-sensitive allele (N^{ts}) (Shellenbarger, 1971) and a viable hypomorphic allele (*facet notchoid* [N^{nd3}]) (Bauer, 1943). In the first set of experiments, *N^{ts};ato-Gal4,UAS-lacZ* larvae were raised in a cycling incubator delivering a 30 min, 34°C heat shock every 8 hr from late L1 through wandering L3. L3 brains were examined for DC defects. We find that reducing *Notch* activity during larval development has no effects on the number, morphology, or position of the DC neurons or on the formation of the commissure (Figure 6A). In contrast, we observed defects in axon branching out of the commissure into the optic lobe. Specifically, we observed excessive branching and defasiculation of the axon bundles entering the optic lobe (Figure 6A, arrows). Importantly, these defects were not rescued by a wild-type copy of *Notch* driven by the *ato* enhancer in the DC (*N^{ts}; UAS-N^{+};ato-Gal4,UAS-lacZ*) (data not shown), suggesting that the requirement for *Notch* in DC axon arborization is nonautonomous in contrast to the requirement for *ato*. Larvae reared under the cycling heat shock paradigm or at a consistent 28°C temperature between either L1 and adult or L3 and adult did not produce homozygous N^{ts} flies. Therefore, to examine the adult DC innervation pattern in a background of reduced *Notch* activity, we used *N^{nd3};ato-Gal4,UAS-lacZ* male flies. As shown in Figure 6B, these flies show excessive branching in the medulla (arrows), resulting in an aberrant innervation pattern similar to that caused by *ato* overexpression in the DC neurons. The disruption is milder due to the fact that N^{nd3} is a weak allele of *Notch*.

Do the defects observed in *Notch* mutants reflect an independent function for *Notch* in arborization? It is possible that the conditions used in this study resulted in mild neurogenic phenotypes generating extra DC target cells. This, in turn, would cause the DC neurons to arborize excessively to innervate new targets. To rule out this possibility, we performed area density (number of cells per unit area) and optic lobe cortex volume (volume occupied by optic lobe cell bodies) analyses on N^{ts} L3 brains and N^{nd3} adult brains. We find that by both criteria, there are no significant differences between wild-type and mutant brains (see Experimental Procedures). Therefore, our data support a model in which *ato* generates the branching pattern by antagonizing *Notch* activity in the DC.

To show that *Notch* function is not required within the DC neurons themselves, we overexpressed a dominant-negative form of *Notch* (*UAS-N^{EC}*) (Jacobsen et al., 1998) using *ato-Gal4*. N^{EC} has no effect on the formation of the larval (data not shown) or adult (Figure 6C) axonal patterns. In contrast, N^{EC} expression in imaginal discs results in strong loss of *Notch* function phenotypes and pupal lethality (data not shown), demonstrating that the construct is active. This shows that while *Notch* function is required specifically for arborization of the DC neurons, its requirement is nonautonomous. The prediction that *ato* represses *Notch* activity in the DC cells implies that gain of *Notch* function within the DC would result in inhibition of axonal branching, a phenotype similar to that of loss of *ato* function. Giniger (1998) has shown that the membrane-bound, wild-type form of *Notch* (N^{+}) is required to rescue the axonal defects associated with the loss of *Notch* function. However, in all cases in which *ato* and *Notch* appear to interact in the PNS, it is the nuclear form of *Notch* that is thought to be involved. To evaluate the effects of the gain of *Notch* function, we overexpressed both forms of *Notch* in the DC neurons: the membrane-bound N^{+} and the nuclear form, N^{intra} (Struhl et al., 1993). We find that overexpression of N^{+} has no effect on the axonal pattern (data not shown), whereas overexpression of N^{intra} results, in comparison with controls (Figure 6D), in a severe inhibition of axonal branching over the lobula and a complete failure of innervation of the medulla (Figure 6E). These data suggest that the nuclear form of *Notch*, but not the membrane-bound form, affects the arborization pattern of the DC axons. Finally, if *ato* suppresses *Notch* signaling within the DC, gain of *Notch* function should be epistatic to the gain of *ato* function, placing *Notch* genetically downstream of *ato*. Therefore, the combined overexpression of *ato* and N^{intra} should result in the same phenotype as the overexpression of N^{intra} alone. Figure 6F shows that brains in which both *ato* and N^{intra} are overexpressed using *ato-Gal4* have a phenotype identical to that of N^{intra} overexpression alone. Taken together, the data presented above support the hypothesis that *ato* acts to suppress *Notch* signaling within the DC and that this suppression is essential for the generation of the proper arborization pattern of the DC axons.

The *ato*-Expressing Neurons Are Essential for Eclosion

What is the function of the *ato*-expressing neurons? To address this question, we overexpressed the cell death gene *reaper* and the cytotoxin Ricin (Moffat et al., 1992; Hidalgo et al., 1995; White et al., 1996) in these cells using the *ato-Gal4* lines 14a and 10. This leads to the loss of all *ato*-expressing cells in the brain (Figure 3H). At 22°C, only 18% of the flies that express the Ricin in the *ato* neurons eclose when compared with their control siblings, although almost all flies develop to the pharate adult stage. At 28°C, none of the flies carrying both constructs hatched. The same observations were made with *reaper* expression using *ato-Gal4* (data not shown). The Ricin and *reaper*-expressing escaper flies showed

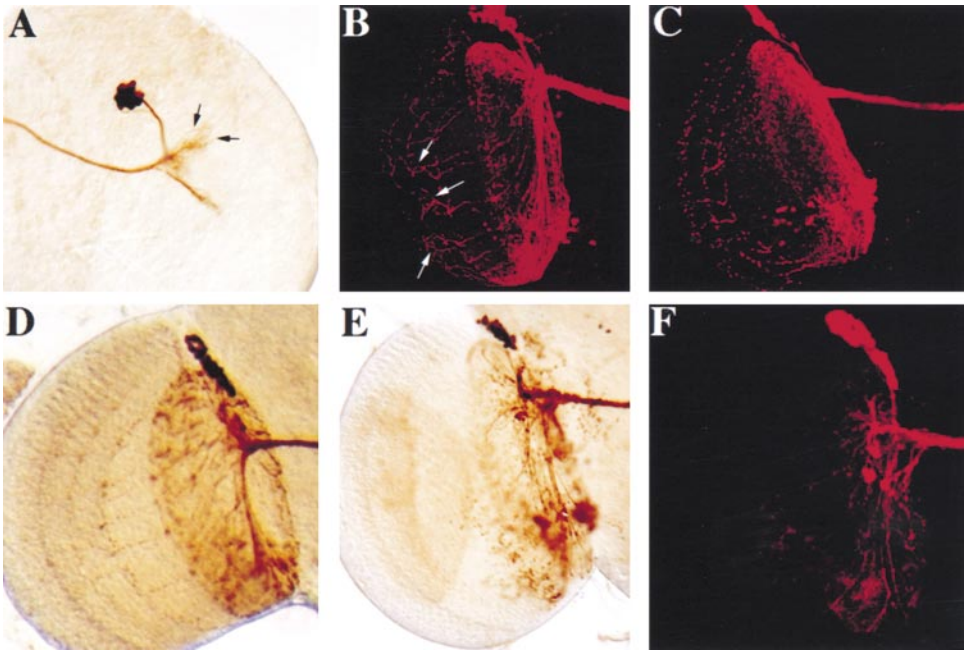

Figure 6. *ato* and *Notch* Interact to Regulate Axon Branching

(A) A N^{ts};*ato-Gal4,UAS-lacZ*/+ L3 brain subjected to multiple heat shocks between L1 and L3, stained for β-gal expression. Reduction of *Notch* activity results in excessive branching out of the commissure. Two defasiculated bundles of axons enter the optic lobe. Arrow points to ectopic bundle.

(B) A confocal section through a N^{md3};*ato-Gal4,UAS-lacZ*/+ brain, showing excessive branching over the medulla (arrows) as a result of reduction in *Notch* activity.

(C) A confocal section through a N^{EC};*ato-Gal4,UAS-lacZ*/+ adult brain stained for β-gal expression. No defects are observed.

(D) A +/*CyO;ato-Gal4,UAS-lacZ*/+ adult brain stained for β-gal expression showing the normal pattern of *ato-Gal4* expression.

(E) A *UAS-*N^{intra}/+;*ato-Gal4,UAS-lacZ*/+ adult brain stained for β-gal expression. Gain of *Notch* function causes a severe reduction in axonal branching over the lobula. No axons cross over to the medulla.

(F) A confocal section through a *UAS-*ato^{1}/*UAS-*N^{intra};*ato-Gal4,UAS-lacZ*/+ adult brain stained for β-gal expression. The defects observed are identical to those seen in *UAS-*N^{intra}/+;*ato-Gal4,UAS-lacZ*/+ brains.

a 2–3 day delay in eclosion compared with control siblings. After hatching, however, they were viable and fertile, and displayed no obvious behavioral defects. In addition, we noted that the overexpression of N^{intra} in the *ato* neurons also resulted in very few adult escapers (10% of expected progeny eclosed, and most die as pharate adults). When pharate adults who failed to hatch after a 5 day delay in the *reaper*, Ricin, and N^{intra} experiments were dissected out of their pupal cases while they were still alive, they failed to move and usually died within 24 hr. These data indicate that the *ato*-expressing cells and their proper arborization are important for proper eclosion. However, it is impossible at this point to distinguish between the requirements for the DC, the VBC, the VLC, or any combination thereof.

Discussion

ato Is Expressed in Many Components of the Visual Pathway

ato is expressed in previously undescribed cells of the central brain. One of the three clusters expressing *ato* in the adult is derived from *ato*-positive cells in the embryonic brain, suggesting that *ato* controls multiple aspects of the development of that lineage. The other two clusters express *ato* de novo in postmitotic neurons. This dynamic pattern of expression has not been documented for other *Drosophila* proneural genes and suggests that *ato* may be used in multiple developmental contexts for different purposes. Perhaps the most intriguing feature of *ato* expression in the brain is that it is localized to cells that connect the brain to both optic lobes via a commissure, and thereby, indirectly, the two optic lobes to each other. Each cluster arborizes both ipsi- and contralaterally onto the optic lobes, perhaps indicative of bilateral communication via the *ato* neurons. *ato* is also expressed in photoreceptors and optic lobes and is required for their development (Jarman et al., 1994, 1995). *ato* is therefore involved in the development of several components of the adult visual pathway, from retina to brain. The DC axons do not connect directly to photoreceptors 1–6 (R1–R6), as we observe no axons in the lamina. In addition, they do not make contact with the R7 and R8 axons, either. Brains from *GMR-GFP/ato-Gal4,UAS-lacZ* flies do not show connections between DC axons and R7 and R8 photoreceptor axons (data not shown), which traverse the lamina to synapse in the medulla (for review, see Kunes, 1999). Attempts to determine which neuronal populations the DC neurons synapse with, using *UAS-WGA* (Yoshihara et al., 1999), were also unsuccessful. Hence, we were unable to determine which type of neurons synapse with the neurons of the DC.

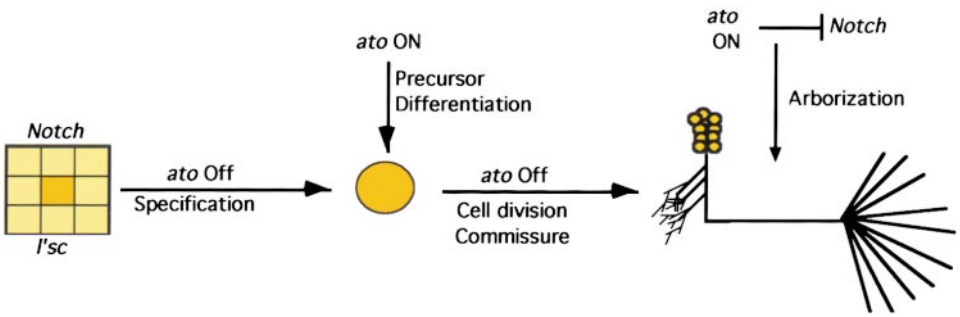

Figure 7. Model for *ato* Function in the Central Brain

ato does not act as a proneural gene in the DC lineage and is therefore not required for neuroblast specification. Rather, it appears to endow precursor cells with a specific differentiation program. Following this, *ato* expression is terminated until cell division within the DC lineage has ceased, the commissure has formed, and axons are beginning to branch out into the optic lobes at the L3 stage. *ato* is then activated to antagonize *Notch* activity within the DC neurons, thereby creating a discrepancy in *Notch* activity between the DC neurons and the surrounding tissue. This would then allow for the stereotyped arborization pattern observed in adults.

The importance of the *ato*-expressing neurons is underscored by the lethal phenotype observed when they are removed by Ricin or *reaper* expression or when they fail to innervate the optic lobes. This is in contrast to mutations that remove or adversely affect large portions of the brain, including the protocerebral bridge, the central complex, and the mushroom bodies (Davis, 1993; Strauss and Heisenberg, 1993). During pupal development, *ato-Gal4* is expressed in ~15 scattered cells, found mainly in the abdomen and thorax, that do not appear to be neurons or muscles (data not shown). While it is unlikely that the loss of these cells is the cause of the lethality observed in *ato-Gal4/UAS-Ricin* flies, we cannot rule out this possibility. Interestingly, lethal mutations in the *optomotor blind* locus (Pflugfelder et al., 1992) cause strong defects in the lobula and also cause pharate adult lethality and eclosion failure. Furthermore, we noted that $ato^{1}/Df(3R)p13$ flies hatched in lower proportions as compared with ato^{1} homozygous flies (15%–25% of expected), which correlates with the severity of the arborization phenotype observed in each case. In summary, the loss of the cells or their failure to innervate the lobula causes eclosion defects.

ato Is Not a Proneural Gene in the Central Brain

To understand the function of *ato* in the embryonic precursors, we used a novel fate mapping strategy. Briefly, this strategy involves the addition of the *UAS-Gal4* step between the *ato-Gal4* and *UAS-lacZ* steps. This resulted in the labeling of the developing DC cells during L1 and L2. Thus, we were able to trace the DC lineage using a single cross and antibody staining. One possible pitfall for this strategy is the possibility that some cells may be able to silence the UAS promoter or degrade the *Gal4* protein. However, to our knowledge, there is no evidence for silencing of the UAS promoter in somatic cells (for a review of the *Gal4* system, see Phelps and Brand, 1998).

The results of the fate mapping experiment show that the DC in the L3 brain arises from *ato*-expressing embryonic precursors and that *ato* is therefore reactivated within the same lineage. Interestingly, in the embryonic brain, *ato* expression initiates well after neuroblast selection and delamination (Younossi-Hartenstein et al., 1997), suggesting that in this context *ato* is not expressed in a proneural cluster. Instead, preselected precursors transiently express *ato*, and, consequently, *ato* cannot be regarded as a proneural gene in this lineage. The DC phenotype in *ato* mutant brains further supports this conclusion. *ato* mutants do not lack neurons of the DC. Rather, subtle differentiation defects are observed at L3. These defects suggest that *ato* is playing a minor and/or redundant role in the differentiation of the DC precursors. These data show conclusively that *ato* is not a proneural gene in this lineage.

Novel Functions for *ato* and *Notch* in the Brain

Loss- and gain-of-function data support the notion that *ato* is required for the proper arborization of the DC axons. In *ato* mutants, defects are observed in the innervation of the lobula complex. Specifically, it appears that the innervation of the lobula complex is severely impaired. These defects cannot be due to the loss of potential signals from the medulla or lobula complex, missing and reduced, respectively, in *ato* mutants. *so* mutant brains lack the medulla and have a reduced lobula complex, similar to *ato* mutants, yet have a wild-type DC axon innervation pattern in the lobula complex. This suggests that the axonal phenotype is caused specifically by the *ato* mutation. The fact that the lobular arborization pattern in *ato* mutants can be rescued by expressing *ato* specifically in brain cells under the control of its own promoter indicates that the requirements for *ato* in arborization are not only specific but also cell autonomous. Overexpression of *ato* in the DC further supports this notion. High levels of *ato* in the DC causes an arborization defect opposite to that observed in the mutants. We conclude that *ato* function is essential for generating the proper innervation pattern observed in wild-type brains.

A clue about the mechanism of *ato* function in axon arborization comes from examining defects associated with the loss and gain of function of *Notch* in the DC. The generalized, but not the DC-specific, reduction in *Notch* activity results specifically in axonal branching defects. These defects are opposite to those observed in the *ato* loss-of-function situation. Furthermore, overexpression of a dominant-negative form of *Notch* in the

DC results in no observable phenotypes. Conversely, overexpression of a constitutively active form causes a phenotype similar to that caused by the loss of function of *ato* and opposite to that caused by the gain of function of *ato*. Hence, the nuclear form of *Notch* interacts with *ato* in the DC neurons. In the absence of *Notch* activity, axonal branching defects are observed as early as L3, suggesting a requirement for *Notch* activity in the optic lobes when axonal branching is initiated. This coincides with the point of *ato* reactivation in the DC lineage. Finally, we find that the interaction between *ato* and *Notch* is antagonistic and that the gain of function of *Notch* in the DC is epistatic to that of *ato*. In agreement with our observations, two recent reports have shown a role for *Notch* signaling in regulation of neurite outgrowth in mammalian neurons (Franklin et al., 1999; Sestan et al., 1999). In conclusion, it appears likely that *ato* regulates DC neurite arborization by modulating *Notch* activity levels.

A model for *ato* and *Notch* Function in the DC Lineage

The data presented above suggest a model in which *ato* plays two distinct functions during DC lineage development (Figure 7). The first function is revealed by examining DC defects in L3. Since *ato* is expressed only in the embryonic precursors of the DC prior to L3, all defects observed at L3 must be due to its requirement in embryos. L3 defects show that *ato* is not required for precursor selection/determination but rather for minor aspects of precursor differentiation. The second function of *ato* involves the organization of the arborization pattern of the DC axons exiting the commissure into the lobula complex. In this role, *ato* acts, at least in part, to antagonize *Notch* signaling within the DC. This may result in a differential of *Notch* activity between the outgrowing DC axons and the potential target cells in the optic lobes. It will be interesting to determine if the regulation of *Notch* activity levels is a common mechanism for the control of axonal branching.

Implications for the Role of bHLH Proteins in Neuronal Lineage Development

Two questions are of interest in the context of the model proposed above. First, do other proneural genes (for example, *scute*) regulate axon patterning or other postmitotic aspects of neuronal differentiation? *scute* is reactivated in the embryonic PNS at stage 14 well after precursor selection. It will be interesting to identify the cells in which *scute* is expressed at stage 14 as a prelude to understanding its postselection function. Second, different mammalian homologs of *ato* act at different points of neuronal lineage development (Cau et al., 1997; Kim et al., 1997; Roztocil et al., 1997; Ahmed et al., 1998; Brown et al., 1998; Ma et al., 1998; Tsuda et al., 1998; Bermingham et al., 1999; Ben-Arie et al., 2000). Whether any of them has a role in neurite development will be interesting to determine.

Experimental Procedures

Fly Strains and Genetics

Most mutant fly strains used in this study have been published and are described and referenced throughout the text. *UAS-lacZ* lines were obtained from the Bloomington stock center. Flies were raised on standard fly food. All crosses involving mutant stocks were performed at 25°C, except crosses involving the temperature-sensitive *Notch* allele (N^{ts}). N^{ts} crosses were set at 18°C and shifted, as indicated in the text, to a cycling heat shock incubator that delivered a 30 min, 34°C heat shock every 8 hr. Crosses using the *UAS-Gal4* system for the purpose of transgene overexpression were set at 22°C and 28°C. *ato-Gal4* transgenic flies were generated by first cloning the *Gal4* cDNA into a modified pCasper vector with a minimal promoter (a gift from D. Eberl) and then cloning the *ato* 3.6 kb BamHI-BglII fragment upstream of the minimal promoter. This construct was injected, and independent transformant lines were isolated. *UAS-Gal4* flies were generated by cloning the *Gal4* cDNA into the pUAST vector, and transformant lines were isolated on different chromosomes. Four lines were combined to generate the multiple insertion line used in this study. Both individual and multiple insertion lines were tested for the absence of expression throughout embryonic and larval development using a *UAS-lacZ* reporter strain.

In Situ Hybridization

In situ hybridization was performed according to Tautz and Pfeifle (1989). Briefly, wild-type *Canton S* embryos were collected and dechorionated in 50% bleach, washed thoroughly with deionized water, and fixed for 20 min in fixation buffer (4% formaldehyde, PBT [1× phosphate-buffered saline (PBS), 0.3% Triton X-100], and 50% heptane). Larval brains were dissected in PBT and fixed in 4% formaldehyde, PBT. *ato* cDNA was transcribed using the nonradioactive RNA labeling kit from Roche Molecular Biochemicals. Labeled RNA was used to hybridize embryos/brains in hybridization solution (Hyb: 50% formamide, 1× PBT). Following hybridization, embryos were washed with decreasing concentrations of Hyb in PBT followed by several washes in PBT. Samples were then incubated with a 1:2000 dilution of alkaline phosphatase– (AP-) conjugated anti-digoxygenin overnight at 4°C. Samples were washed and visualized with AP substrates (nitroblue tetrazolium chloride, 5-bromo-4-chloro-3-indolylphosphate toluidinium).

Immunohistochemistry

Immunohistochemistry was performed according to Mardon et al. (1994). Adult brains were dissected from heads in PBT and fixed with 4% formaldehyde in PBT for 15–20 min. Fixed embryos (see above) and adult brains were incubated in 1× PAXDG buffer (PBT, 5% normal goat serum, 1% bovine serum albumin, 0.1% deoxycholate, and 1% Triton X-100) overnight either with anti-β-gal (Promega, 1:2000) or guinea pig (GP) anti-ATO (see below; 1:1000 for diaminobenzidine staining, 1:200 for fluorescent staining). Samples were washed with PAXDG and incubated with the appropriate secondary antibodies at 1:250. Detection was performed either with the ABC kit (Vectastain) or with fluorescent secondary antibodies (Jackson). For fluorescent staining, washes were extended to 4 hr instead of 1. Cryosections were made and stained according to Buchner and Hofbauer (Ashburner, 1989). Confocal sections were obtained using a BioRad 1024 confocal microscope.

GP Anti-ATO Antibody

An EcoRI-HindIII fragment encoding the full-length *ato* ORF was cloned into the pET 28a+ expression vector (Novagen). The bHLH domain was deleted by a BamHI digest. The resulting *ato*Δ fragment was expressed as a His tag fusion protein. Soluble ATOΔ protein was purified according to His tag kit specifications (Novagen), and 2 mg of protein were used to immunize guinea pigs.

Area Density and Volume Calculations

Whole-mount larval and adult brains were fixed with 4% formaldehyde in 1× PBT, treated with 50 μg/ml DNAse-free RNAse, and stained with 50 μg/ml propidium Iodide. Area density (number of cells per unit area) was calculated as follows: 5 μm confocal sections of different optic lobe regions were taken at 100× magnification in-frame of 100 μm × 100 μm. The number of cells within each frame was counted for 20 sections per brain region, averaged, and divided by the frame area. In the inner proliferation center, this number ranged from 0.021 to 0.023 cells/μm^2 for N^{ts} L3 brains ($n = 6$). For wild-type L3 brains, the number ranged from 0.020 to 0.024 cells/

μm^2. Volumes were calculated by taking 5 μm sections through an entire brain region at 16× magnification, calculating the area of the region of interest within each section (NIH Image 1.66), adding the areas of all sections, and multiplying by section depth ($n = 5$). For N^{nd3} adult brains, the average density in the medulla was 0.022 cells/μm^2 and 0.023 cells/μm^2 for wild-type controls ($n = 7$). No significant difference in volume between wild-type and mutant brains was observed ($V_{Nts}/V_{wt} = 0.984$; $V_{wt}/V_{Nnd3} = 1.103$).

Acknowledgments

We thank R. Yao for technical assistance. B. H. is indebted to K. Schulze for help with frozen sections and P. Callaerts for lessons in dissecting whole brains. We are grateful for reagents and flies from A. Jarman, E. Giniger, M. Baylies, D. Eberl, P. Taghert, L. Zipursky, C. Desplan, M. Muskavitch, H. Okano, A. Brand, P. Fernandez-Funez, and J. Botas. P. R. Hiesinger and K. F. Fischbach generated the three-dimensional images available on the World Wide Web. We thank K. Choi, G. Mardon, P. Callaerts, and R. Hiesinger for comments. Thanks to I. Meinertzhagen and members of the Bellen lab, particularly Karen Schulze, for helpful discussions. This work was supported by a National Institutes of Health postdoctoral fellowship to B. A. H. and a National Aeronautics and Space Administration grant to H. J. B. and H. Y. Z. N. B. is an associate and Y.-N. J., H. Y. Z., and H. J. B. are Howard Hughes Medical Institute Investigators.

Received October 18, 1999; revised January 24, 2000.

References

Ahmed, I., Acharya, H.R., Rogers, J.A., Shibata, A., Smithgall, T.E., and Dooley, C.M. (1998). The role of NeuroD as a differentiation factor in the mammalian retina. J. Mol. Neurosci. *11*, 165–178.

Akazawa, C., Ishibashi, M., Shimizu, C., Nakanishi, S., and Kageyama, R. (1995). A mammalian helix–loop–helix factor structurally related to the product of *Drosophila* proneural gene *atonal* is a positive transcriptional regulator expressed in the developing nervous system. J. Biol. Chem. *270*, 8730–8738.

Ashburner, M. (1989). *Drosophila*: A Laboratory Manual (Cold Spring Harbor, NY: Cold Spring Harbor Laboratory Press).

Bauer, H. (1943). Eine neue Mutation *facet-notchoid* bei *Drosophila melanogaster* und die Deutung des notch-Effektes. Z. indukt. Abstamm.-u. VererbLehre *81*, 374–390.

Bausenwein, B., Dittrich, A.P.M., and Fischbach, K.F. (1992). The optic lobe of *Drosophila melanogaster*. Cell Tissue Res. *267*, 17–28.

Ben-Arie, N., McCall, A., Berkman, S., Eichele, G., Bellen, H.J., and Zoghbi, H.Y. (1996). Evolutionary conservation of sequence and expression of the bHLH protein ATONAL suggests that it plays a role in neurogenesis. Hum. Mol. Genet. *5*, 1207–1216.

Ben-Arie, N., Bellen, H.J., Armstrong, D.L., McCall, A.E., Gordadze, P.R., Guo, Q., Matzuk, M.M., and Zoghbi, H.Y. (1997). Math1 is essential for genesis of cerebellar granule neurons. Nature *390*, 169–172.

Ben-Arie, N., Hassan, B.A., Bermingham, N.A., Armstrong, D., Matzuk, M., Bellen, H.J., and Zoghbi, H.Y. (2000). Functional conservation of *atonal* and *Math1* in the CNS and PNS. Development *127*, 1039–1048.

Bermingham, N.A., Hassan, B.A., Price, S.D., Vollrath, M.A., Ben-Arie, N., Eatock, R.A., Bellen, H.J., Lysakowski, A., and Zoghbi, H.Y. (1999). *Math1*, an essential gene for the generation of inner ear hair cells. Science *284*, 1837–1841.

Brand, A.H., and Perrimon, N. (1993). Targeted gene expression as a means of altering cell fates and generating dominant phenotypes. Development *118*, 401–415.

Brown, N.L., Kanekar, S., Vetter, M.L., Tucker, P.K., Gemza, D.L., and Glaser, T. (1998). Math5 encodes a murine basic helix–loop–helix transcription factor expressed during early stages of retinal neurogenesis. Development *125*, 4821–4833.

Cau, E., Gradwohl, G., Fode, C., and Guillemot, F. (1997). Mash1 activates a cascade of bHLH regulators in olfactory neuron progenitors. Dev. Suppl. *124*, 1611–1621.

Clark, I.E., Jan, L.Y., and Jan, Y.N. (1997). Reciprocal localization of Nod and kinesin fusion proteins indicates microtubule polarity in the *Drosophila* oocyte, epithelium, neuron and muscle. Development *124*, 461–470.

Daniel, A., Dumstrei, K., Lengyel, J.A., and Hartenstein, V. (1999). The control of cell fate in the embryonic visual system by atonal, tailless and EGFR signaling. Development *126*, 2945–2954.

Davis, R.L. (1993). Mushroom bodies and Drosophila learning. Neuron *11*, 1–14.

Dreller, C., and Kirschner, W.H. (1993). Hearing in honeybees: localization of the auditory sense organ. J. Comp. Physiol. A *173*, 275–279.

Eberl, D.F. (1999). Feeling the vibes: chordotonal mechanisms in insect hearing. Curr. Opin. Neurobiol. *9*, 389–393.

Fischbach, K.F. (1981). Neurons in the optic lobes of the *Drosophila* mutant *sine oculis*. Neurosci. Lett. *7*, S288.

Franklin, J.L., Berechid, B.E., Cutting, F.B., Presente, A., Chambers, C.B., Foltz, D.R., Ferreira, A., and Nye, J.S. (1999). Autonomous and non-autonomous regulation of mammalian neurite development by notch 1 and delta 1. Curr. Biol. *9*, 1448–1457.

Giniger, E. (1998). A role for *Abl* in *Notch* signaling. Neuron *20*, 667–681.

Giniger, E., Jan, L.Y., and Jan, Y.N. (1993). Specifying the path of the intersegmental nerve of the Drosophila embryo: a role for *Delta* and *Notch*. Development *117*, 431–440.

Hidalgo, A., Urban, J., and Brand, A.H. (1995). Targeted ablation of glia disrupts axon tract formation in the *Drosophila* CNS. Development *121*, 3703–3712.

Jacobsen, T.L., Brennan, K., Arias, A.M., and Muskavitch, M.A. (1998). Cis-interactions between *Delta* and *Notch* modulate neurogenic signaling in *Drosophila*. Development *125*, 4531–4540.

Jarman, A.P., and Ahmed, I. (1998). The specificity of proneural genes in determining *Drosophila* sense organ identity. Mech. Dev. *76*, 117–125.

Jarman, A.P., Grau, Y., Jan, L.Y., and Jan, Y.N. (1993). *atonal* is a proneural gene that directs chordotonal organ formation in the *Drosophila* peripheral nervous system. Cell *73*, 1307–1321.

Jarman, A.P., Grell, E.H., Ackerman, L., Jan, L.Y., and Jan, Y.N. (1994). *atonal* is the proneural gene for *Drosophila* photoreceptors. Nature *369*, 398–400.

Jarman, A.P., Sun, Y., Jan, L.Y., and Jan, Y.N. (1995). Role of the proneural gene, *atonal*, in formation of *Drosophila* chordotonal organs and photoreceptors. Development *121*, 2019–2030.

Kim, P., Helms, A.W., Johnson, J.E., and Zimmerman, K. (1997). XATH-1, a vertebrate homolog of *Drosophila atonal*, induces a neuronal differentiation within ectodermal progenitors. Dev. Biol. *187*, 1–12.

Kolb, B., and Whishaw, I.Q. (1998). Brain plasticity and behavior. Annu. Rev. Psychol. *49*, 43–64.

Kunes, S. (1999). Stop or go in the target zone. Neuron *22*, 639–640.

Ma, Q., Chen, Z., del Barco Barrantes, I., de la Pompa, J.L., and Anderson, D.J. (1998). Neurogenin1 is essential for the determination of neuronal precursors for proximal cranial sensory ganglia. Neuron *20*, 469–482.

Mardon, G., Solomon, N.M., and Rubin, G.M. (1994). *dachshund* encodes a nuclear protein required for normal eye and leg development in *Drosophila*. Development *120*, 3473–3486.

McIver, S.B. (1985). Mechanoreception. In Comprehensive Insect Physiology, Biochemistry and Pharmacology, L.I. Gilbert and D.A. Kerkut, eds. (New York: Pergamon Press), pp. 71–132.

Moffat, K.G., Gould, J.H., Smith, H.K., and O'Kane, C.J. (1992). Inducible cell ablation in *Drosophila* by cold-sensitive ricin A chain. Development *114*, 681–687.

Moulins, M. (1976). Ultrastructure of Chordotonal Organs, P.J. Mill, ed. (London: Chapman and Hall).

Nieto, M.A. (1996). Molecular biology of axon guidance. Neuron *6*, 1039–1048.

Okabe, M., and Okano, H. (1997). Two-step induction of chordotonal organ precursors in *Drosophila* embryogenesis. Development *124*, 1045–1053.

Pflugfelder, G.O., Roth, H., Poeck, B., Kerscher, S., Schwarz, H., Jonschker, B., and Heisenberg, M. (1992). The lethal(1)optomotor-blind gene of Drosophila melanogaster is a major organizer of optic lobe development: isolation and characterization of the gene. Proc. Natl. Acad. Sci. USA *89*, 1199–1203.

Phelps, C.B., and Brand, A.H. (1998). Ectopic expression in *Drosophila* using *Gal4* system. Methods Enzymol. *14*, 367–379.

Roztocil, T., Matter, S.L., Alliod, C., Ballivet, M., and Matter, J.M. (1997). NeuroM, a neural helix–loop–helix transcription factor, defines a new transition stage in neurogenesis. Development *124*, 3263–3272.

Sestan, N., Artavanis-Tsakonas, S., and Rakic, P. (1999). Contact-dependent inhibition of cortical neurite growth mediated by notch signaling. Science *286*, 741–746.

Shellenbarger, D.L. (1971). A temperature-sensitive *Notch* mutant of *Drosophila melanogaster*. Genetics *68*, 61–62.

Strausfeld, N.J. (1976). Atlas of an Insect Brain (Berlin: Springer-Verlag).

Strauss, R., and Heisenberg, M. (1993). A higher control center of locomotor behavior in the *Drosophila* brain. J. Neurosci. *13*, 1852–1861.

Struhl, G., Fitzgerald, K., and Greenwald, I. (1993). Intrinsic activity of the *Lin-12* and *Notch* intracellular domains in vivo. Cell *74*, 331–345.

Sun, Y., Jan, L.Y., and Jan, Y.N. (1998). Transcriptional regulation of *atonal* during development of the *Drosophila* peripheral nervous system. Development *125*, 3731–3740.

Takebayashi, K., Takahashi, S., Yokota, C., Tsuda, H., Nakanishi, S., Asashima, M., and Kageyama, R. (1997). Conversion of ectoderm into a neural fate by ATH-3, a vertebrate basic helix–loop–helix gene homologous to *Drosophila* proneural gene *atonal*. EMBO J. *16*, 384–395.

Tautz, D., and Pfeifle, C.A. (1989). Non-radioactive in situ hybridization method for the localization of specific RNAs in *Drosophila* embryos reveals translational control of the segmentation gene *hunchback*. Chromosoma *98*, 81–85.

Tessier-Lavigne, M., and Goodman, C.S. (1996). The molecular biology of axon guidance. Science *274*, 1123–1133.

Tsuda, H., Takebayashi, K., Nakanishi, S., and Kageyama, R. (1998). Structure and promoter analysis of *Math3* gene, a mouse homolog of *Drosophila* proneural gene *atonal*. Neural-specific expression by dual promoter elements. J. Biol. Chem. *273*, 6327–6333.

White, K., Tahaoglu, E., and Steller, H. (1996). Cell killing by the *Drosophila* gene *reaper*. Science *271*, 805–807.

Yang, M.Y., Armstrong, J.D., Vilinsky, I., Strausfeld, N.J., and Kaiser, K. (1995). Subdivision of the *Drosophila* mushroom bodies by enhancer-trap expression patterns. Neuron *15*, 45–54.

Yoshihara, Y., Mizuno, T., Nakahira, M., Kawasaki, M., Watanabe, Y., Kagamiyama, H., Jishage, K.I., Ueda, O., Suzuki, H., Tabuchi, K., et al. (1999). A genetic approach to visualization of multisynaptic neural pathways using plant lectin transgene. Neuron *22*, 33–41.

Younossi-Hartenstein, A., Green, P., Liaw, G.J., Rudolph, K., Lengyel, J., and Hartenstein, V. (1997). Control of early neurogenesis of the Drosophila brain by the head gap genes *tll*, *otd*, *ems*, and *btd*. Dev. Biol. *182*, 270–283.

Zhao, C., and Emmons, S.W. (1995). A transcription factor controlling development of peripheral sense organs in *C. elegans*. Nature *373*, 74–78.

zur Lage, P., and Jarman, A.P. (1999). Antagonism of EGFR and *Notch* signaling in the reiterative recruitment of *Drosophila* adult chordotonal sense organ precursors. Development *126*, 3149–3157.

zur Lage, P., Jan, Y.N., and Jarman, A.P. (1997). Requirement for EGF receptor signaling in neural recruitment during formation of *Drosophila* chordotonal sense organ clusters. Curr. Biol. *7*, 166–175.